

The submillimetre dielectric response of a PLZT 9.5/65/35 relaxor thin film

This article has been downloaded from IOPscience. Please scroll down to see the full text article.

1997 J. Phys.: Condens. Matter 9 5205

(<http://iopscience.iop.org/0953-8984/9/24/017>)

View [the table of contents for this issue](#), or go to the [journal homepage](#) for more

Download details:

IP Address: 171.66.16.207

The article was downloaded on 14/05/2010 at 08:58

Please note that [terms and conditions apply](#).

The submillimetre dielectric response of a PLZT 9.5/65/35 relaxor thin film

I Fedorov†, J Petzelt†, V Železný†, A A Volkov‡, M Kosec§ and U Delalut§

† Institute of Physics, Czech Academy of Science, Na Slovance 2, 18040 Praha 8, Czech Republic

‡ Institute of General Physics, Russian Academy of Science, Vavilova 38, 117942 Moscow, Russia

§ 'Jožef Stefan' Institute, University of Ljubljana, Jamova 39, 1001 Ljubljana, Slovenia

Received 7 October 1996, in final form 12 February 1997

Abstract. We report on the first quantitative evaluation of the soft-mode behaviour of the relaxor PLZT 9.5/65/35. The transmission spectra of a PLZT thin film deposited on a sapphire substrate were measured in the 4–350 cm^{-1} region at temperatures from 300 up to 523 K, and in the 15–350 cm^{-1} range at 8–300 K. We fitted the spectra using the model of classical oscillators, and calculated the parameters of the observed lattice modes. The results were compared with those for bulk ceramics, and satisfactory agreement was achieved. The soft mode is heavily damped, and below room temperature it shows a strong hardening on cooling. Above room temperature, its eigenfrequency levels off, but the corresponding dielectric loss maximum continues to soften weakly down to $\sim 33 \text{ cm}^{-1}$ at 523 K, where the mode becomes overdamped. The lower-frequency data require an additional relaxation below the measured range. Comparison of all of the available data at room temperature points to strong polydispersive losses in the 10^{10} – 10^{12} Hz range, and another dispersion region at lower frequencies. We assign them to fluctuations of the polar nanocluster volume, and to reorientations of the cluster polarization, respectively. Their contribution to the low-frequency permittivity is much stronger than that of the soft mode.

1. Introduction

Transparent ceramics of $(\text{Pb}_{1-x}\text{La}_x)(\text{Zr}_y\text{Ti}_{1-y})\text{O}_3$ (PLZT 100($x/y/1-y$)) have been thoroughly studied since their discovery in 1971, mainly because they are frequently used in electro-optic, piezoelectric, and other applications [1].

For sufficiently high La concentration (depending on the Zr/Ti ratio) their dielectric properties exhibit a typical relaxor behaviour [2], characterized by broad frequency-dependent maxima in both parts of the temperature-dependent complex dielectric response $\epsilon^*(T, \omega) = \epsilon'(T, \omega) - i\epsilon''(T, \omega)$. Their macroscopic symmetry remains paraelectric cubic over the whole temperature range (unless an external bias field is applied), but clear evidence was found for the formation of nanosized polar clusters below the hypothetical ferroelectric Curie temperature for the same Zr/Ti composition without La doping (PZT-100($1-y$)) [3]. This nanoscopically inhomogeneous phase shows many features similar to those of dipolar glasses [2, 4], including broad and complex dielectric dispersion. However, due to a very high value of the permittivity ($\epsilon' \sim 10^4$), only few studies exist on the high-frequency dielectric dispersion of the relaxor PLZT [5–9].

Kersten *et al* [5] observed a single relaxation between 10^3 and 10^{10} Hz in PLZT 8/65/35. On decreasing the temperature from 500 K to 400 K, the relaxation rate follows

the Arrhenius slowing down, which extrapolates to ~ 60 MHz at 300 K. In a sample of the same composition, Schmitt and Dorr [6] observed a relaxation at much lower frequency, between 10^5 and 10^7 Hz (at 300 K, the relaxation frequency $\omega_r \sim 1$ MHz), which slows down according to the power law $\omega_r = A(T - T_c)^2 + C$, with $A = 1.7 \times 10^2$ Hz K $^{-2}$, $T_c \approx 400$ K, and $C \approx 1.6 \times 10^6$ Hz for $400 < T < 530$ K. Even if the low-frequency permittivity data below 10^5 Hz do not differ dramatically for the two cases, the aforementioned dielectric dispersion does, but the reason for this was not discussed (reference [5] was not cited in [6]).

In the far-infrared (FIR) range, Lurio and Burns [7] measured the reflectivity of PLZT 12/40/60 and 9/65/35 at 300 K and 470 K, obtaining no significant variations in the reflectivity spectra. From a four-oscillator fit, they obtained the complex dielectric response function in the polar phonon range ($50\text{--}1000$ cm $^{-1}$), with large uncertainty concerning the parameters of the lowest polar phonon, which plays the role of the soft mode in ferroelectric perovskites.

The FIR reflectivity of PLZT 9.75/65/35 was more thoroughly measured by Železný *et al* [8]. By combining their data with room temperature transmission data in the $8\text{--}18$ cm $^{-1}$ range (obtained using a backward-wave-oscillator (BWO) spectrometer), they were able to separate two contributions to the submillimetre (SMM) dispersion: one from the heavily damped lowest polar mode near 40 cm $^{-1}$, and another from an additional relaxation near 10 cm $^{-1}$. Both characteristic frequencies showed weak softening on heating, but no quantitative conclusions could be drawn.

The reflectivity data are not sensitive enough for the SMM dielectric response and the soft-mode behaviour to be analysed for relaxor ferroelectrics. Due to the high absorption, obtaining transmission data is feasible only for very thin plates, with thickness of the order of 1 μm . Such thicknesses are now readily available, produced using thin-film techniques, but no SMM transmission data on PLZT thin films have been published so far. It should be noted that despite several Raman studies having been made of the relaxor PLZT [7, 9–11], the behaviour of the soft mode could not be determined due to its weakness, high damping, and overlapping with the quasielastic component.

Several papers were published on the processing and dielectric properties of relaxor PLZT films [12–16]. The low-frequency dielectric permittivity is strongly dependent on the processing conditions, and is always smaller than for bulk ceramics. Also its temperature dependence is smoother, and the permittivity maximum (Curie temperature) in films is shifted to higher temperatures with respect to that for bulk ceramics [16]. No data on the frequency dispersion of the permittivity of the relaxor PLZT films are available. In this paper we present the first quantitative soft-mode study of a PLZT 9.5/65/35 film and bulk ceramic, and discuss the high-frequency dielectric dispersion in these samples.

2. Experiment

In order to prepare a stoichiometric PLZT 9.5/65/35 film, we used a starting solution with 10 mol% excess of PbO. This should compensate the PbO weight losses during the annealing [17, 18]. Anhydrous lead acetate, anhydrous lanthanum acetate, zirconium *n*-propoxide, and titanium *n*-propoxide were used as precursors, and 2-methoxyethanol as a solvent. The acetates were dried prior to use. The solid contents of the alkoxides and one of the acetates after drying were determined gravimetrically. The precursors were weighed and mixed with 2-methoxyethanol in a dry box. The acetates were reacted by dissolving upon heating, and stirring. After dissolving them, the clear yellow solution was refluxed for two hours at 118 °C, and then distilled under normal pressure to obtain the sol concentration

of 0.5 mol l^{-1} . The sol was cooled to room temperature, and then 4 vol% of formamide was added. The synthesis was carried out under a dried argon atmosphere. The coating was carried out on a sapphire substrate 0.3 mm thick by the spin-coating technique in the ambient atmosphere. The substrate was aligned with the optic axis perpendicular to the surface so that it was optically isotropic in the plane. First 0.0625 M sol of PbTiO_3 prepared identically to the PLZT was spun at 3000 rpm for 60 seconds, pyrolysed at 350°C for 60 seconds, and annealed at 550°C for 20 minutes. Afterwards, the PLZT film, consisting of five layers, was deposited by spinning it at 3000 rpm for 60 seconds. Each deposition step was followed by pyrolysis at 350°C for 60 seconds. The film was put in a hot furnace, and was fired for 20 hours at 600°C in air. During the firing, the crystalline perovskite phase is quickly formed from the amorphous phase. The main Pb loss is expected to occur at the beginning of firing from the amorphous phase, because of the very low PbO vapour pressure above the perovskite phase [18]. The film thickness ($139 \pm 5 \text{ nm}$) and stoichiometry were determined using Rutherford back-scattering (RBS). The good stoichiometry (within 1 at.%) of the film was confirmed.

The infrared transmittance spectra of the PLZT 9.5/65/35 film deposited on the sapphire substrate were measured using two different pieces of equipment. The data for the frequency range $4\text{--}23 \text{ cm}^{-1}$ were obtained using BWO spectroscopy [19]. The measurements were carried out in the temperature region between 300 K and 523 K. For higher frequencies, we used the Fourier transform infrared technique (FTIR). The measurements were done using a Fourier spectrometer, Bruker IFS 113v. The transmittance spectra were obtained for the frequency range $25\text{--}350 \text{ cm}^{-1}$ (limited by the sapphire opacity) at temperatures of 300–523 K. The Fourier spectrometer was also used for measurements at low temperatures (8–100 K). For detection in the $15\text{--}100 \text{ cm}^{-1}$ region, we used a helium-cooled Ge bolometer.

After merging the BWO and FTIR data, at temperatures 8–100 K we obtained the transmittance spectra for the frequency range $15\text{--}350 \text{ cm}^{-1}$, and between 300 K and 523 K we obtained the spectra for the frequency range $4\text{--}350 \text{ cm}^{-1}$. The merged spectra were then used for the fitting procedure.

3. Results and evaluation

The transmittance spectra of the PLZT 9.5/65/35 thin film on the sapphire substrate measured at various temperatures using the FTIR technique are presented in figure 1. The oscillations in the spectra are due to the interference of the radiation inside the sapphire substrate [20]. The arrows in figure 1 point to the frequencies of the transverse thin-film phonons. From figure 1 it can be seen that the low-frequency phonon mode softens as the temperature increases, but its frequency levels off at higher temperatures. The position of the high-frequency mode is practically temperature independent (the hard mode).

Performing the fitting procedure, we calculated the frequency dependence of the transmission coefficient of a model system consisting of two slabs (a thin-film–substrate system). In order to determine the optical constants of sapphire, we carried out similar measurements (see the previous section) on a bare sapphire substrate.

To fit our spectra, we first tried a model of two classical damped harmonic oscillators:

$$\epsilon_0(\omega) = \epsilon_\infty + \frac{\Delta\epsilon_s \omega_s^2}{\omega_s^2 - \omega^2 + i\omega\gamma_s} + \frac{\Delta\epsilon_h \omega_h^2}{\omega_h^2 - \omega^2 + i\omega\gamma_h} \quad (1)$$

where ϵ_∞ represents the sum of the dielectric contributions of the higher-frequency optical phonons and the electronic polarizability, ω_s and ω_h are the eigenfrequency of the soft mode and of the hard mode, respectively, γ_s and γ_h their damping, and $\Delta\epsilon_s$ and $\Delta\epsilon_h$ their dielectric

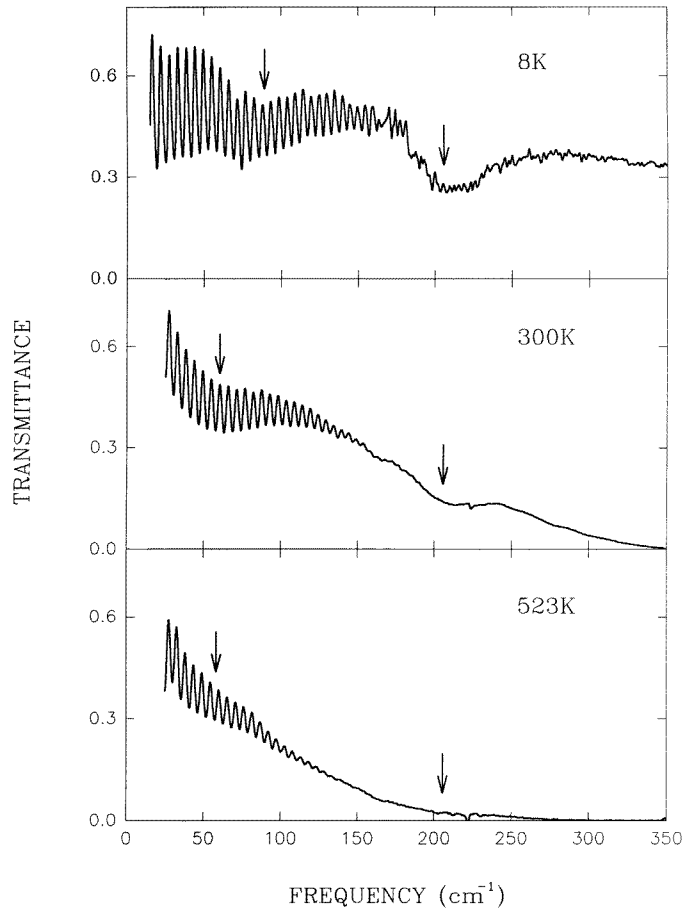


Figure 1. The temperature dependence of the FTIR transmission spectra. The arrows show the fitted phonon mode frequencies.

strength, respectively. Figure 2 shows the room temperature transmittance, together with the fit for the soft-mode region (below 100 cm^{-1}) obtained with the following parameters: $\omega_s = 60.5\text{ cm}^{-1}$, $\gamma_s = 94\text{ cm}^{-1}$, $\Delta\epsilon_s = 212$, $\omega_h = 206\text{ cm}^{-1}$, $\gamma_h = 37\text{ cm}^{-1}$, and $\Delta\epsilon_h = 11$. $\epsilon_\infty = 9.5$ was fixed from the known data on bulk ceramics [7, 21, 9]. The quality of the fit for the range above 25 cm^{-1} (FTIR) is not good near the interference minima. This effect is caused mainly by the so-called secondary interferogram effects, produced by the radiation reflected from the sample back to the interferometer, and, after being reflected from the interferometer mirrors, contributing to the original beam passing through the sample. As the reflected intensity is maximal at the frequencies of the transmission minima, this spurious effect is most pronounced there, and is negligible near the transmission maxima. This effect can be reduced by tilting the sample. Another cause of the decrease in the interference amplitude is the finite divergence of the incident beam. This effect, however, influences the interference maxima as well as the minima, and becomes noticeable at the high-frequency end only.

Another systematic deviation of the fit from the data is seen in the low-frequency BWO data near the interference maxima. This is not a spurious instrumental effect, but provides

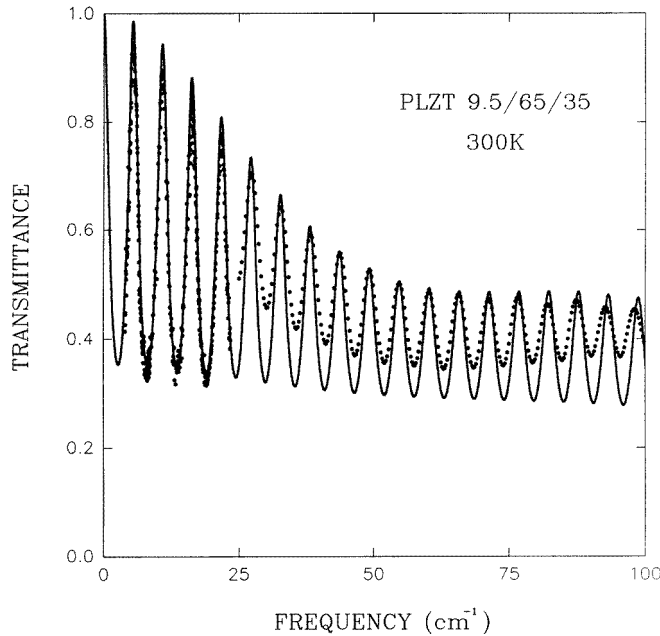


Figure 2. The room temperature transmittance of the PLZT–sapphire system. The oscillations in the spectrum are due to the interference of the radiation inside the sapphire substrate. The dots are the experimental points, and the full line is the model fit (see the text). The data for below 25 cm^{-1} were taken from the BWO spectrometer, and the data for above 25 cm^{-1} from the Bruker IFS 113v.

evidence of additional absorption in this range. This can be most simply accounted for by a Debye relaxation contribution added to equation (1):

$$\epsilon(\omega) = \epsilon_r(\omega) + \epsilon_0(\omega) \quad \epsilon_r(\omega) = \frac{\Delta\epsilon_r \omega_r}{\omega_r + i\omega}. \quad (2)$$

The fits showed that the maximum value of ω_r which can fit our data well is $\omega_r = 19 \text{ cm}^{-1}$ (with $\Delta\epsilon_r = 270$). However, the resulting low-frequency permittivity (~ 345) is probably too small. A more realistic value of ω_r , which should account for the value of the low-frequency permittivity, should be appreciably smaller, and depend strongly on the value of the low-frequency permittivity, which cannot be directly determined for our sample without electrodes. Taking the opposite extreme case, namely its value for bulk ceramics (about 2800 [7]), fitted together with SMM data, requires $\omega_r \approx 0.2 \text{ cm}^{-1}$ (6 GHz) and $\Delta\epsilon_r \approx 2600$. The quality of this fit is comparable to that of the previous one with $\omega_r = 19 \text{ cm}^{-1}$. In figure 3 we show the BWO data at room temperature (the low-frequency part of figure 2) with two fits: without the Debye relaxation (dotted line), and with the $\omega_r = 0.2 \text{ cm}^{-1}$ relaxation (full line).

It is important to note that the optimum soft-mode parameters ($\omega_s = 60.5 \text{ cm}^{-1}$, $\gamma_s = 95 \text{ cm}^{-1}$, $\Delta\epsilon_s = 195$) in the case of the fit with the $\omega_r = 0.2 \text{ cm}^{-1}$ relaxation included do not strongly differ from those listed before. In the case of the best fit, where the $\omega_r = 19 \text{ cm}^{-1}$ relaxation is included, the soft-mode parameters are as follows: $\omega_s = 60.5 \text{ cm}^{-1}$, $\gamma_s = 62 \text{ cm}^{-1}$, $\Delta\epsilon_s = 54$. It is seen from the three sets of parameters that the soft-mode frequency is independent of the presence of the relaxation, and its accuracy is quite high. The relaxation can somewhat influence the soft-mode strength and damping,

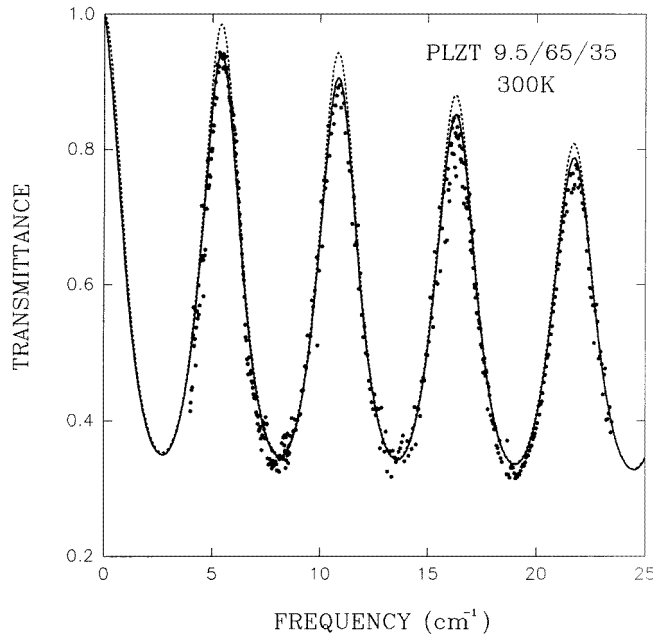


Figure 3. The BWO part from the spectrum in figure 2, fitted with (full line) and without (broken line) the presence of a low-frequency Debye relaxation (see the text).

but only in the case of its highest acceptable frequency. This is understandable, because in this case there is a strong overlapping of the relaxation mode with the heavily damped soft mode.

For fitting the data at other temperatures, we used the Debye relaxation with fixed $\omega_r = 0.2 \text{ cm}^{-1}$, and the value of $\Delta\epsilon_r$ was taken in such a way that the sum of all of the mode contributions was equal to the experimental value of the low-frequency permittivity [7]. We are aware of the fact that the constant- ω_r approximation is not realistic. In fact, one could expect an Arrhenius-like softening of ω_r on cooling [5]. However, this has a negligible effect on our fitted soft-mode parameters. Moreover, we found no experimental permittivity data for low temperatures $T < 100 \text{ K}$. Therefore our low-temperature relaxation parameters serve merely as a qualitative illustration (see later, in figure 5).

The temperature dependence of the soft-mode parameters is shown in figure 4. For comparison, the parameters obtained from the fit of the bulk reflectivity [9] (see the discussion, in section 4) are also plotted in figure 4 (broken lines). As the temperature increases, the soft-mode frequency first decreases from 85.5 cm^{-1} at 8 K to 58 cm^{-1} at 373 K, but remains constant at higher temperatures. Its dielectric strength increases monotonically from ~ 90 at 8 K to ~ 240 at 523 K; the damping also displays a similar behaviour. At high temperatures, the soft mode is almost overdamped ($\gamma_s \approx 2\omega_s$), and the maximum of the dielectric loss function $\epsilon''(\omega)$ appears near $\omega_s^2/\gamma_s \approx 33 \text{ cm}^{-1}$, i.e. substantially lower than ω_s . This is more compatible with the bulk reflectivity data (see the discussion, in section 4). The soft oscillator strength $f_s = \Delta\epsilon_s \omega_s^2$ (proportional to the effective charge squared) is only weakly temperature dependent: it increases monotonically from $6.5 \times 10^5 \text{ cm}^{-2}$ at 8 K to $8.1 \times 10^5 \text{ cm}^{-2}$ at 523 K. Note also that the hard-mode parameters are practically temperature independent: $\omega_h = 206 \text{ cm}^{-1}$ is constant, and γ_h and

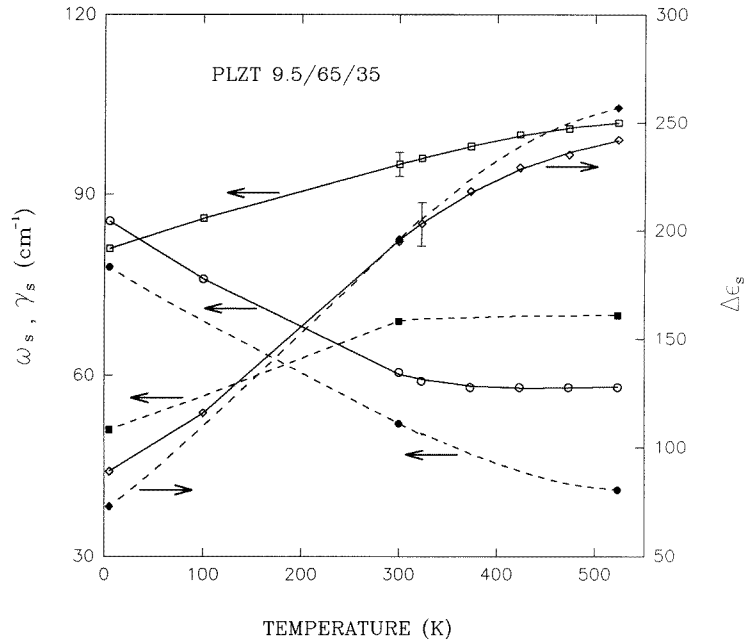


Figure 4. The lowest (soft-) polar mode parameters of PLZT 9.5/65/35 as a function of the temperature. Circles, squares, and diamonds denote the eigenfrequency, the damping, and the dielectric strength, respectively. Open symbols—thin-film data; full symbols—bulk reflectivity data (see figure 6).

$\Delta\epsilon_h$ increase only slightly from 33 and 10.5 at 8 K to 38 and 11.3 at 523 K, respectively. The temperature dependences of the dielectric strengths of both modes, and the total low-frequency permittivity (which is practically indistinguishable from the strong relaxational contribution, on our logarithmic scale) are shown in figure 5.

4. Discussion

First we would like to check to what extent the thin-film data are compatible with the IR response of bulk ceramics. To do this, we have fitted the IR reflectivity of bulk PLZT 9.5/65/35 measured in our previous work [9] with a model of four generalized oscillators (the factorized form of the dielectric function [22]):

$$\epsilon(\omega) = \epsilon_\infty \prod_j \frac{\omega_{jLO}^2 + i\omega\gamma_{jLO} - \omega^2}{\omega_{jTO}^2 + i\omega\gamma_{jTO} - \omega^2} \quad (3)$$

where ω_{jTO} , ω_{jLO} and γ_{jTO} , γ_{jLO} represent the frequencies and the dampings of the transverse and longitudinal modes, respectively. The results of the fit are shown in figure 6. Note the generally weak temperature dependence, which is a consequence of the glassy nature of this relaxor ceramic below room temperature (the freezing temperature $T_f \approx 240$ K—see later). The soft-mode parameters from our fit are rather inaccurate, because the low-frequency wing of the reflectivity cannot be well fitted. The complex dielectric function calculated from our film data is compared with the one from the bulk ceramic data in figure 7. The agreement of the two data fits is reasonable. Only the soft-

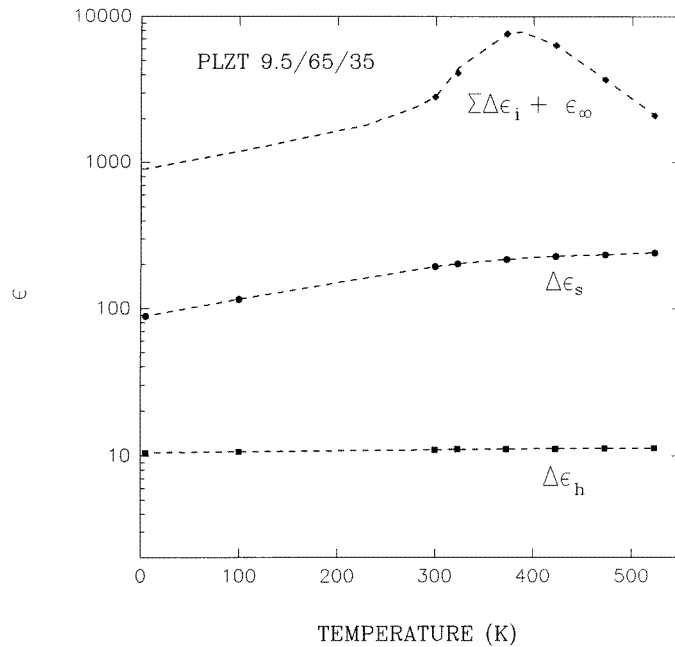


Figure 5. Temperature dependences of the dielectric strength of the soft mode and of the hard mode near 206 cm^{-1} , and the temperature dependence of the sum of all of the dielectric contributions, which is adjusted to the fit of the low-frequency permittivity above room temperature [7]. The dielectric strength $\Delta\epsilon_r$ of the relaxation is practically indistinguishable from the last curve.

mode damping seems to be definitely larger in the case of the film. This indicates some inhomogeneity in the film sample, or influence of surface effects.

The most striking behaviour concerns the levelling off of the soft-mode frequency above room temperature (figure 4). The subsequent lack of any anomaly near the maximum of the low-frequency permittivity (for bulk ceramics $T_{max} \approx 380 \text{ K}$; for thin films $T_{max} \approx 430 \text{ K}$ [16]) had already been noticed [8]. In fact, this is expected, because the maximum in $\epsilon'(T)$ is not connected with any change of symmetry or phase in the case of relaxor ferroelectrics. It is now quite clear that it is caused by a kinetic effect, and by the freezing of polar nanoregions which will be discussed below. The lack of any softening at higher temperatures is only a partly apparent effect, because the increasing damping causes further softening of the loss $\epsilon''(\omega)$ maximum, which, in the case of heavily damped and overdamped excitations, is a more physical quantity than the eigenfrequency [23]. It seems that the loss maximum softens partly towards the Burns temperature $T_d \approx 620 \text{ K}$, where the local phase transition (in nanoregions poor in La) starts [21], but the degree of softening (probably incomplete) and the behaviour above T_d would require studies at higher temperatures on thicker films, including the SMM wave range.

The soft-mode hardening below room temperature seems to reflect the local mode hardening in individual frozen polar clusters. A similar or even more pronounced hardening on cooling would be expected if the ferroelectric phase were induced by a bias field. Such experiments have not been performed yet. The origin of the microwave dispersion, which seems to be present at all temperatures in the relaxor ferroelectric PLZT, is obviously connected with the formation of nanoscopic polar clusters below the Curie temperature of

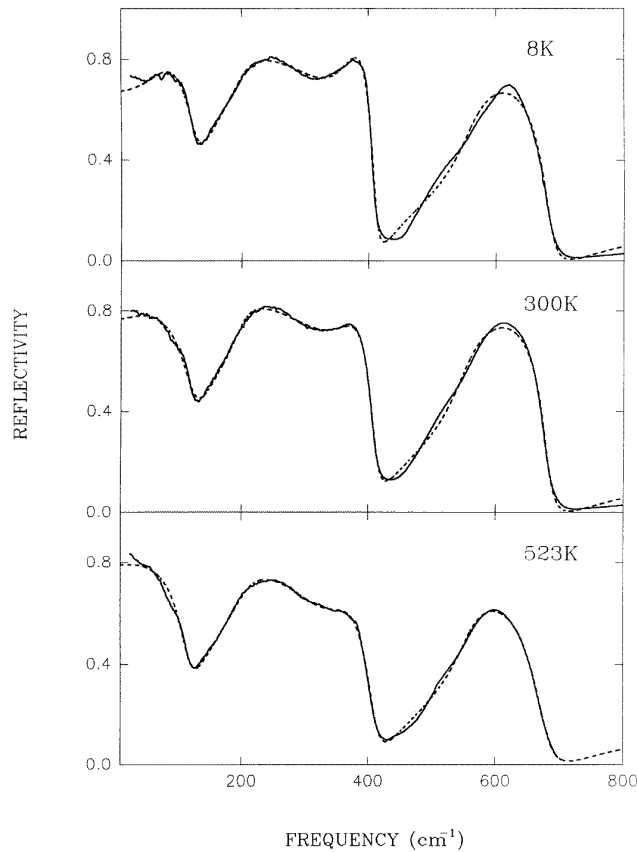


Figure 6. The IR reflectivity of the bulk PLZT 9.5/65/35 hot-pressed ceramic (full lines), and its fit (see the text—broken lines). The experimental data are taken from reference [9].

the corresponding pure PZT without La doping ($T_d \approx 620$ K) [21]. These clusters are nucleated first in nanoregions poor in La, where the local phase transition temperature is expected to be as high as T_d . On combining all of our experiments (IR bulk reflectivity, FIR film transmission, and SMM thin-plate transmission [8], 10, 30, and 100 GHz waveguide measurements [24]), and the earlier low-frequency permittivity measurements [7], it becomes clear that the additional dielectric dispersion below the soft-phonon-mode response at room temperature is much broader than a single Debye relaxation. The dielectric loss seems to be practically constant between 10 and 300 GHz, reaching a high value $\epsilon'' \sim 300$ to 400; and the permittivity ϵ' drops from ~ 1000 at 10 GHz to ~ 300 at 300 GHz. This is a manifestation of a polydispersive behaviour with the distribution of relaxation frequencies, which is at least two decades wide.

At room temperature, PLZT 9.5/65/35 is well below the low-frequency permittivity maximum, but well above the freezing temperature, where the remanent polarization in a previously poled sample vanishes ($T_f \approx 240$ K) [25]. In this temperature range one can suppose that the structure consists of a dense system of uncorrelated polar nanoclusters which are still dynamic, i.e. their dipole moments undergo time fluctuations, including flipping into other orientations. This motion is expected to slow down as T_f is approached, and freezes below T_f . At room temperature it should be connected with the lower-frequency dispersion

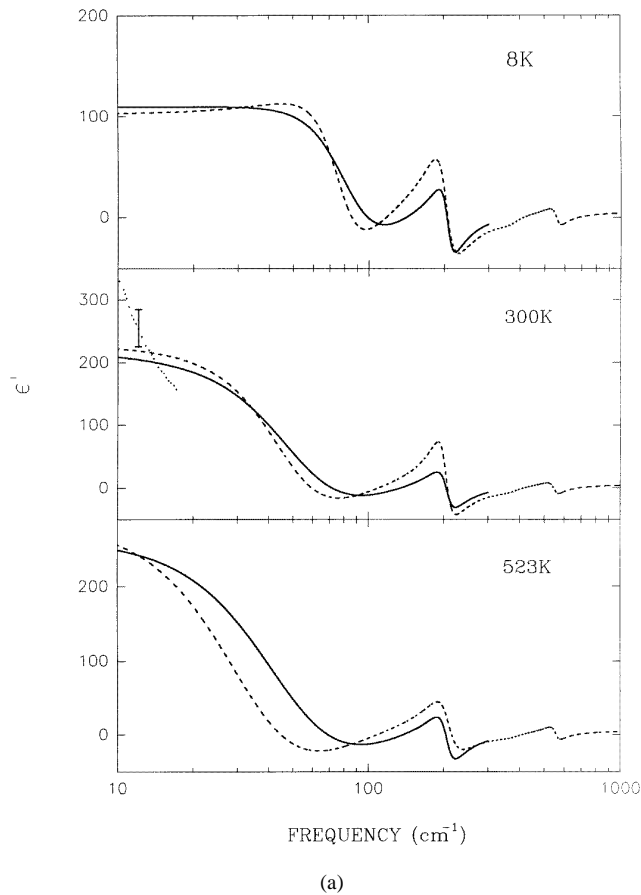


Figure 7. The dielectric function of PLZT 9.5/65/35 calculated from the fit of the thin-film data (full lines) compared to that from the fit of the bulk reflectivity (broken lines). (a) Real part, and (b) imaginary part. The dotted lines show the SMM data from reference [8].

already observed in the 10^5 – 10^8 Hz range [5, 6, 25, 26]. However, there exists another type of fluctuation which must be strongly dielectrically active, namely the fluctuations of the cluster volume or, in other words, the vibrations of the charged intercluster boundaries. This situation is in full analogy to the domain wall motion in normal polydomain ferroelectrics, or to the infrared-active phason in incommensurate ferroelectrics (discommensuration motion), where the above-mentioned type of fluctuation is known to contribute strongly to the dielectric response [27]. In analogy to the domain wall motion, the motion of intercluster boundaries is expected to be thermally activated. It contributes to the dielectric response at any temperature below T_f , and, of course, also above T_f , as long as the lifetime of the clusters is sufficiently high. We suggest that the high-frequency dispersion (10^{10} – 10^{12} Hz) in relaxor PLZT at room temperature is mainly due to this motion. To prove this hypothesis, it would be worthwhile to carry out wide-band dielectric spectroscopy, especially at room temperature and below it, to prove the existence of the two expected dispersion regions, and to establish their temperature behaviours.

It should be noticed that pronounced dielectric relaxations in the 10^3 – 10^8 Hz range have been frequently observed even in the paraelectric cubic phases of perovskites.

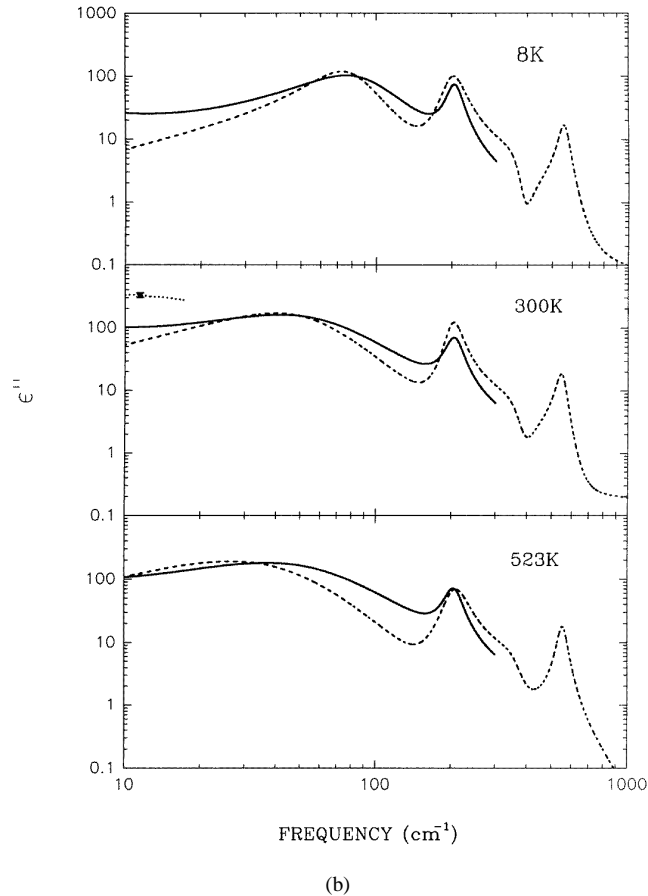


Figure 7. (Continued)

At higher temperatures this is suggested to be connected with space charges localized at grain boundaries (in the case of ceramics), or at sample surfaces [28]. At lower temperatures, polaronic hopping of charged point defects becomes more important [28]. This represents other mechanisms, which could be also responsible for the low-frequency dielectric dispersion in relaxor materials.

In the picture that we suggest applying near to and below room temperature, when the relaxor structure is full of long-living polar nanoclusters, we have to assign our soft mode to fluctuations of the cluster polarization amplitude. This is also in full analogy to incommensurate ferroelectrics, where one mode from the amplitudon branch (whose wavevector equals that of the incommensurate wave) is strongly IR active [27]. The high damping down to low temperatures can be then understood as an inhomogeneous broadening due to the distribution of cluster sizes.

5. Conclusions

The first quantitative FIR study was performed on a PLZT 9.5/65/35 thin film and bulk ceramic. The temperature behaviour of the soft mode was evaluated and discussed.

On heating from 8 K, the soft mode shows a softening which slows down above room temperature, and the soft mode becomes overdamped. Except for the higher damping, the thin-film data are in agreement with the bulk reflectivity data. Moreover, they yield detailed information on the mode frequency behaviour which is directly observable in the spectra. A pronounced broad dispersion was found below the soft-mode response in the 10^{10} – 10^{12} Hz range at room temperature, which was tentatively assigned to volume fluctuations of the polar nanoclusters. This gives a higher contribution to the low-frequency permittivity than that of the soft mode.

Acknowledgments

The authors are indebted to V Peřina for performing the RBS measurements. The work was supported by the Grant Agency of the Czech Republic (project No 202/95/1393), and by the Grant Agency of the Czech Academy of Sciences (project No A1010604).

References

- [1] Haertling G H 1987 *Ferroelectrics* **75** 25
- [2] Dai X, Xu Z and Viehland 1994 *Phil. Mag. B* **70** 33
- [3] Burns G 1985 *Phase Transitions* **5** 261
- [4] Hochli U T, Knorr K and Loidl A 1990 *Adv. Phys.* **39** 405
- [5] Kersten O, Rost A and Schmidt G 1983 *Phys. Status Solidi a* **75** 495
- [6] Schmitt H and Dorr A 1989 *Ferroelectrics* **93** 309
- [7] Lurio A and Burns G 1974 *J. Appl. Phys.* **45** 1986
- [8] Železný V, Petzelt J, Volkov A A and Ozolinsh M 1990 *Ferroelectrics* **109** 149
- [9] Pokorný J, Petzelt J, Gregora I, Železný V, Vorliček V, Zikmund Z, Fedorov I, Pronin A and Kosec M 1996 *Ferroelectrics* **186** 115
- [10] Brya W J 1971 *Phys. Rev. Lett.* **26** 1114
- [11] Dellis J-L, Dallennes J, Carpentier J-L, Morell A and Farhi R 1994 *J. Phys.: Condens. Matter* **6** 5161
- [12] Okudaira T, Hachisuka A, Soyama N, Ogi K, Arima H, Matsukawa T and Horie K 1991 *Int. Conf. on Solid State Devices and Materials (Yokohama, 1991)* abstracts, p 204
- [13] Sudhama C, Kim J, Chikarmane V, Lee J C, Tasch A F, Myers E R and Novak S 1992 *Mater. Res. Soc. Symp. Proc.* **243** 147
- [14] Tani T and Payne D A 1994 *J. Am. Ceram. Soc.* **77** 1242
- [15] Teowee G, Quackenbush E L, Baertlein C D, Boulton J M, Kneer E A and Uhlmann D R 1995 *Mater. Res. Soc. Symp. Proc.* **361** 433
- [16] Dausch D E and Haertling G H 1996 *J. Mater. Sci.* **31** 3409
- [17] Reaney I M, Brooks K, Klissurska R, Pawlaczyk C and Setter N 1994 *J. Am. Ceram. Soc.* **77** 1209
- [18] Sato E, Huang Y, Kosec M, Bell A and Setter N 1994 *Appl. Phys. Lett.* **65** 2678
- [19] Volkov A A, Kozlov G V and Prokhorov A M 1989 *Infrared Phys.* **29** 747
- [20] Fedorov I, Petzelt J, Železný V, Komandin G A, Volkov A A, Brooks K, Huang Y and Setter N 1995 *J. Phys.: Condens. Matter* **7** 4313
- [21] Burns G and Dacol F H 1983 *Phys. Rev. B* **28** 2527
- [22] Gervais F 1983 *Infrared and Millimeter Waves* vol 8, ed K J Button (London: Academic)
- [23] Petzelt J, Kozlov G V and Volkov A A 1987 *Ferroelectrics* **73** 101
- [24] Kamba S, Petzelt J, Pokorný J, Endal J and Koukal V 1996 *Proc. 26th European Microelectronics Conf. (Prague, 1996)* (New York: Nexus Information Technology) p 669
- [25] Viehland D, Jang S J, Cross L E and Wuttig M 1991 *J. Appl. Phys.* **69** 6595
- [26] Dimza V J 1996 *J. Phys.: Condens. Matter* **8** 2887
- [27] Petzelt J 1981 *Phase Transitions* **2** 155
- [28] Maglione M 1996 *Ferroelectrics* **176** 1